12th IFAC International Symposium on
Advanced Control of Chemical Processes
July 14-17, 2024. Toronto, Canada

Towards non-invasive quality monitoring and control of stem cell-derived pancreatic islet manufacturing

Rohan Singh * **Hamid Ebrahimi Orimi** **
Praveen Kumar Raju Pedabaliyarasimhuni **
Corinne Hoesli ** **Moncef Chioua** ***

* *Department of Chemical Engineering, Polytechnique Montréal, 2500, Chemin de Polytechnique, H3T 1J4, Montréal, Canada (e-mail: rohan.singh@polymtl.ca).*
** *Department of Chemical Engineering, McGill University, 845 Sherbrooke St W,H3A 0G4, Montréal, Canada*
*** *Department of Chemical Engineering, Polytechnique Montréal, 2500, Chemin de Polytechnique, H3T 1J4, Montréal, Canada (e-mail: moncef.chioua@polymtl.ca).*

Abstract:
Quality monitoring is important for biomanufacturing and often the methods used in laboratory setting do not translate well to industrial setting. In this regard, we present a non-invasive quality control method for classification of well differentiated cells from poorly differentiated ones that is scalable and can be used in online setting for adherent culture systems. The method was implemented on stage 4 of pluripotent stem cell differentiation into beta cells and we use textural analysis to extract features from phase contrast microscopic (PCM) images which were used to train our classifier that achieved an accuracy of 94.04 %. These preliminary findings show promise for its application in the area of processes monitoring in bio-reactors.

Keywords: Adaptive and Learning Systems; Estimation and Robust Estimation; Machine Learning Assisted Modeling

1. INTRODUCTION

The industrialization of stem cell production to generate beta cells holds significant promise for the treatment of diabetes and the mass production of insulin (Docherty and Sussel (2021), Wallner et al. (2018)). Bioreactors, in particular, have emerged as a key technology in this endeavor, providing an environment conducive to the large-scale cultivation and differentiation of stem cells (Almezel (2021), Zhang et al. (2017)).

Quality control (QC) is a critical aspect of this process, ensuring the identity, quality, and safety of the cells (Vaes et al. (2012)).The process of stem cell differentiation into pancreatic islet cells is a complex multi-step process involving several differentiation stages from Stage-1 to Stage-7 (Pagliuca et al. (2014)). Stage 4, where stem cells commit to the pancreatic lineage and become pancreatic progenitor cells (PPCs), is a critical milestone (Kahan et al. (2003)). The presence of specific markers such as PDX1 and NKX6.1 guides this transformation (Aigha and Abdelalim (2020), Aigha et al. (2018)). Currently, flow cytometry is a widely used technique in laboratories for QC, offering a robust method for analyzing cell properties (Nicotra et al. (2020)). However, this method has its limitations. Flow cytometry requires fresh and intact cells, and the process requires specialized equipment and trained operators. Moreover, it requires a sample to be kept separately to perform flow cytometry. Therefore, a part of the product is lost to QC by flow cytometry which is particularly problematic given the already low yield of the process (Manohar et al. (2021)). Finally another solution is to have a smaller culture on the side to do flow cytometry on this, but it may not be representative of the main culture. Generally, laboratories either culture the cells on surfaces, or they culture them in suspension. Most research laboratories currently culture them adherently at least until stage 4, and real-time monitoring of the conditions of the cultures is highly limited. Here, real-time monitoring means observing the changes in culture in an ongoing differentiation process.

In light of these challenges, there is a pressing need for non-invasive, efficient, and scalable QC methods. This study contributes to addressing this gap by exploring the use of textural features from phase contrast microscopic (PCM) images and machine learning for non-invasive QC that can be implemented in an online setting. In this context, "on-line setting" refers to a system where the quality control process is integrated into the production line and operates in real-time. This means that the machine learning model can analyze the PCM images and make decisions about the quality of the product instantly, without interrupting the manufacturing process, allowing for immediate feed-back and correction, potentially saving time and resources. (Visschedijk et al. (2005)).

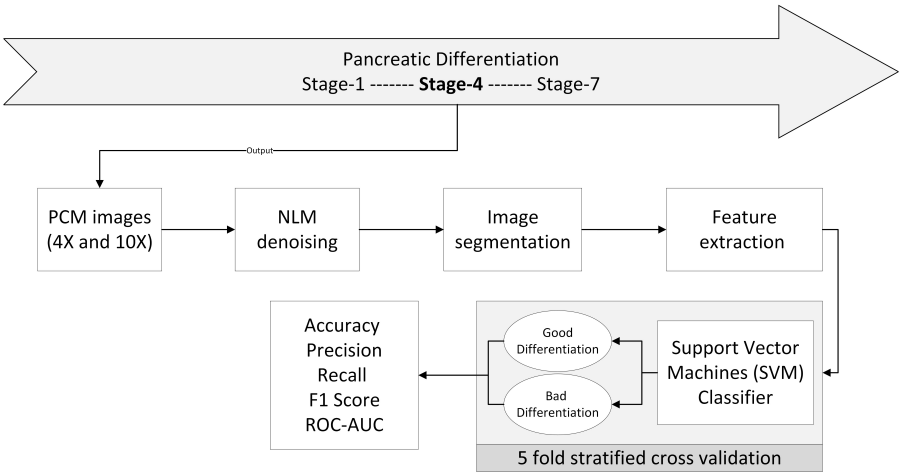

Fig. 1. Proposed methodology used in this study on stage 4 cells, including preprocessing, image processing, feature extraction and postprocessing

Image processing is a crucial component in the field of biomedical research and clinical medicine. It involves the acquisition and analysis of images to visualize anatomical structures, assess the functionality of human organs, point out pathological regions, analyze biological and metabolic processes, set therapy plans, and carry out image-guided surgery among other things (Maddalena and Antonelli (2024)). Image processing significantly enhances the accuracy and efficiency of tumor detection by aiding in the precise segmentation of medical images and extraction of suspicious regions such as tumors (Kapoor and Thakur (2017)). Texture analysis plays a crucial role in a variety of computer vision tasks, including object recognition, surface defect detection, pattern recognition, and medical image analysis (Armi and Fekri-Ershad (2019)). The primary aim of texture analysis is to create features that can effectively categorize textured images. Recent research has highlighted the effectiveness of combinational methods (Liu et al. (2016)) for texture analysis. These methods, which do not fit neatly into any specific category, prioritize discrimination performance, computational complexity, and resistance to challenges such as noise and rotation. In the context of classification, several algorithms have been employed for texture image classification. Notable papers in this field include (Wang et al. (2020)),which proposed a deep learning network for image classification that is based on very basic data processing components: cascaded principal component analysis (PCA), binary hashing, and blockwise histograms , and (Chan et al. (2015)), that introduced a simple deep learning network for image classification, called the PCA network (PCANet), which is based on cascaded PCA, binary hashing, and blockwise histograms. Furthermore, advancements have been made in utilizing morphological openings in a preprocessing stage for improved deep learning (Maetschke et al. (2017)). However, these established methods also demand dataset size to be much larger compared to size of dataset that was available to us. Hence, they were not applicable in our study.

Imaging and texture analysis have the potential to be done in real-time not just at stage 4 but even for earlier stages by analyzing textural features in those stages. The primary benefit of implementing it in earlier stages is that it will allow laboratories or bio-reactors to discontinue the batches that are not meeting acceptance criteria, and therefore it could lead to significant cost savings both during research and development and during manufacturing.

The main contributions of this paper are - 1) We proposed a novel feature extraction methodology based on textural analysis of PCM images. 2) We present preliminary results of SVM based classifier trained on extracted textural features that shows potential to be scalable and used in an online setting.

The rest of the paper is organized in the following manner: Section 2 introduces the proposed methodology based on textural analysis of PCM culture images for feature extraction. Section 3 presents the results of classification of stem cell differentiation based on the extracted features. Section 4 discusses the obtained results, and Section 5 concludes the paper.

2. METHODOLOGY

This study's methodology included data acquisition and preprocessing, image segmentation, feature extraction, and machine-learning-based classification. This process helped accurately identify and distinguish stage 4 pancreatic progenitor cells (PPCs), hence providing useful information about the cell differentiation process. The results obtained from this study lay down the framework for non-invasive classification of PPC from stage 4 PCM images. The workflow of the proposed approach is illustrated in Figure 1. Each step of the methodology is detailed in the following subsections.

2.1 Data Acquisition and Preprocessing

This study used images of stage 4 cells cultures of pancreatic differentiation. 79 four times magnified (4X) and 141 ten times magnified (10X) PCM images were collected for textural analysis and feature extraction.

In preprocessing, images were denoised to enable better textural analysis and feature extraction. The Non-Local

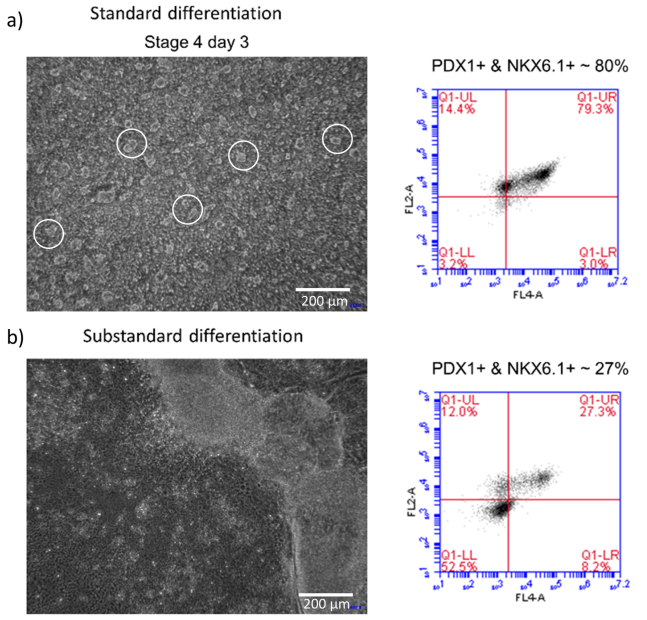

Fig. 2. Phase contrast microscopy images of inter-cell voids at stage 4 for 79% and 27% of PDX1+ and NKX6.1+ (a, b). It shows correlation of inter-cell voids with standard differentiation validated by flow cytometry results.

Means method, a common image processing technique for noise reduction (Buades et al. (2011)), was used for this denoising process.

2.2 Feature selection

The presence of inter-cell voids, as shown in Figure (2 a and b), throughout the culture on day 3 and day 4 of stage 4 of pancreatic differentiation, showed a correlation with higher PDX1 and NKX6.1 presence. This was validated through flow cytometry (Figure 3). PDX1 and NKX6.1 are marker genes for PPCs. Furthermore, the absence of inter-cell voids has been demonstrated and illustrated in the Figure 2.b and Figure 2.c where PDX1 and NKX6.1 secretion is not observed. Because of this correlation of inter-cell voids with presence of PDX1 and NKX6.1 , the features chosen for this analysis were the number of inter-cell voids, the area covered by inter-cell voids, the percentage of area covered by inter-cell voids, the uniformity of inter-cell voids distribution and mean inter-cell voids size. These features were easy to extract after segmentation and helped quantify the quantify the correlation of inter-cell voids with presence of PDX1 and NKX6.1 and enabled the machine learning model to make predictions. Uniformity, in this study, is a measure that shows the level of evenness in the distribution of inter-cell voids across the image area. It is calculated as the ratio of the number of inter-cell voids to the image area, which has been normalized by dividing by 10,000 in our case. A higher uniformity value means a more even spread of inter-cell voids throughout the image, while a lower value indicates an uneven or clustered distribution. Images that met the criterion in Figure 2 a) were labelled as standard while images similar to the one represented in Figure 2 b) were labelled as substandard.

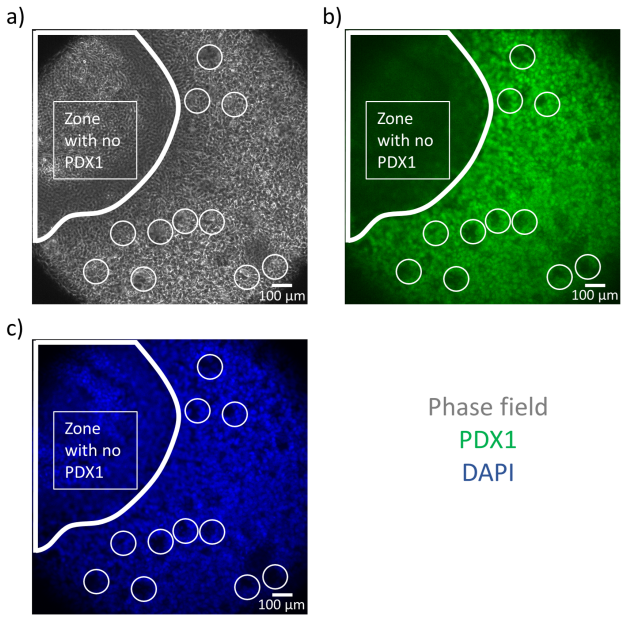

Fig. 3. Phase contrast Microscopy image (a) of stage 4 cells stained by PDX1 marker (b) and DAPI (c); there is no inter-cell voids in the domain with no PDX1

2.3 Image Segmentation

After denoising, the preprocessed images underwent a segmentation process, as described in (Van der Walt et al. (2014)). The goal of image segmentation was to separate and outline areas of interest, specifically, the inter-cell voids in the PCM culture images. Local adaptive thresholding method was used for this purpose (Roy et al. (2014)). This method allowed us to adjust the threshold values for each image region, which helped in extracting relevant features with better precision because the collected PCM images often had variable lighting.

2.4 Feature Extraction

After segmentation, a connected component analysis, as described in (He et al. (2017)), was performed on the segments to extract key features from the segmented areas. The features - number of inter-cell voids, area covered by inter-cell voids, percentage of area covered by inter-cell voids, the uniformity of inter-cell voids distribution and mean inter-cell voids size were used to train our machine learning model for identifying standard differentiation. Below is a pseudocode representing how features were extracted.

```
Algorithm: Extract Cell Cluster Features

Input: image_path, min_cluster_area,
max_cluster_area
Output: num_clusters, total_area,
percentage_area_covered,
uniformity, mean_cluster_size

1: Load image in grayscale.
2: Define 'segment_clusters' function.
3: Inside 'segment_clusters':
   - Apply adaptive histogram equalization.
```

```
   - Apply adaptive thresholding.
   - Find connected components.
   - Initialize 'cluster_areas' list.
   - For each label, calculate area.
   - If area is within range,
   append to 'cluster_areas'.
   - Return number of clusters,
   total area, and image area.
4: Call 'segment_clusters' with image.
5: Calculate percentage area covered:
   - percentage_area_covered =
   (total_area / image_area) * 100
6: Calculate uniformity:
   - uniformity =
   num_clusters / (image_area / 10000)
7: Calculate mean cluster size:
   - mean_cluster_size =
   total_area / num_clusters
8: Return all calculated values.
```

2.5 Correcting class imbalances

Class imbalances were present in our PCM image dataset. We had 30 standard differentiation images and 49 substandard differentiation images for 4X magnification. Similarly, we had 39 standard differentiation images and 102 substandard differentiation images for 10X magnification. To address this class imbalance issue, we used oversampling. Oversampling involves adding artificial samples to the minority class by duplicating existing examples or generating synthetic ones. In this study, Synthetic Minority Oversampling Technique (SMOTE) (Chawla et al. (2002)) was used for oversampling. SMOTE creates synthetic examples by interpolating between the nearest neighbors of the minority class. It helps to increase the diversity and representativeness of the minority class.

2.6 Support Vector Machine (SVM) based Classification

The extracted features were then utilized as input data for a Support Vector Machine (SVM) based classifier. SVM is a robust and widely used machine learning algorithm known for its ability to delineate patterns and classify data points into distinct categories (Chauhan et al. (2019)) . In our study, it was employed to classify between well-differentiated and poorly-differentiated instances based on the acquired feature set. SVM is known to be effective in performing generalization on smaller datasets (Vapnik (1999)). Convolutional neural networks (Li et al. (2014)) have traditionally performed well in image classification tasks but due to the small size of our dataset, we could not use them.

2.7 Performance Metrics

The SVM classifier's performance was evaluated using five-fold stratified cross-validation method (Berrar et al. (2019)). In five-fold cross-validation, the dataset was split into five parts, with four parts used for training and the fifth part used for testing. The splits were rotated and training and testing was performed 4 more times. This validation method ensured that the classifier's performance was thoroughly checked and could be generalized to new data. The evaluation criteria included several performance metrics, such as accuracy, F1 scores, ROC-AUC scores, recall, and precision. These performance metrics gave a complete evaluation of the classifier's ability to differentiate between the two classes of differentiation.

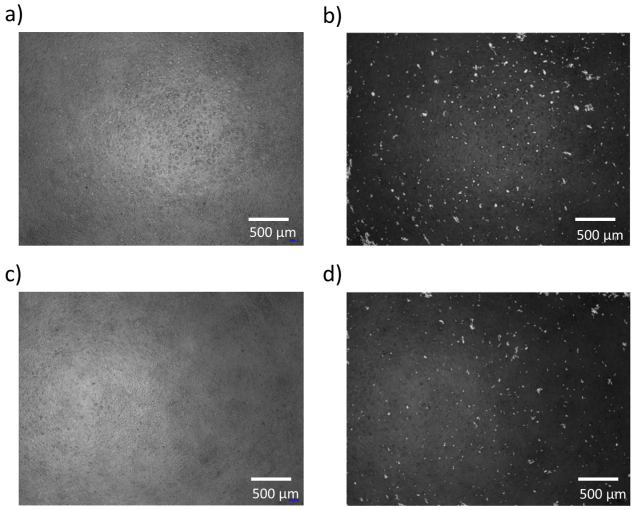

Fig. 4. Original phase contrast microscopy images of cells at stage 4 along with the processed images for standard (a and b) and substandard (c and d) differentiation. It shows a larger number of inter-cell voids uniformly distributed throughout the culture for standard differentiation compared to substandard differentiation

3. RESULTS

In this section, we present the results we obtained using the proposed methodology discussed in previous section. Table 1 compiles the information about the features extracted from Figures 4 (a) and (b) and Figures 4 (c) and (d). We can observe the contrast in the values of featured extracted for standard differentiation compared to substandard differentiation. Table 1 and Figure 4 are representation example of how the features were used to make the classification decision. Similar feature extraction was done for every image in 4X and 10X dataset and these extracted features were used to train the SVM classifier.

Tables 2 and Table 3 summarize the obtained performance metrics values for (4X) and (10X) images for balanced and unbalanced datasets. The performance metrics are average values obtained during cross validation. Except recall, values for the performance metrics are higher for 4X images in comparison to 10X images. We can also observe that the values of the metics for balanced oversampled dataset is not much different from the unbalanced dataset.

Table 1. standard vs. sub-standard differentiation features comparison

Features	standard	sub-standard
No. of inter-cell voids	896	660
area covered (pixels)	43026	24684
percentage area covered	2.24	1.29
Uniformity	4.67	3.44
Mean inter-cell voids size (pixels)	48.02	37.40

Table 2. Cross validation average values for 4X PCM images

Performance Metrics	4X	4X (Oversampled)
Accuracy	0.94	0.92
F1 score	0.91	0.89
ROC-AUC	0.97	0.97
Recall	0.87	0.89
Precision	0.97	0.97

Table 3. Cross validation average values for 10X PCM images

Performance Metrics	10X	10X (Oversampled)
Accuracy	0.89	0.88
F1 score	0.80	0.79
ROC-AUC	0.88	0.90
Recall	0.82	0.85
Precision	0.80	0.76

4. DISCUSSION

In Section 4, we will discuss the results presented in the last section.

Table 1 compiles the information extracted from Figure 4. The features related to the number of inter-cell voids, the area they cover in pixels, and the corresponding percentage show a distinct contrast for standard and substandard differentiation. Specifically, the well-differentiated samples have higher values for all three of these features, indicating a larger presence and distribution of inter-cell voids within their images. On the other hand, the poorly-differentiated examples have significantly lower values in these areas, suggesting a reduced presence and coverage of inter-cell voids. We also considered two additional features: the uniformity of inter-cell voids and the average inter-cell voids size. Our analysis shows that well-differentiated examples tend to have higher uniformity values, further emphasizing the uniform distribution of inter-cell voids within their images.

On the other hand, the average inter-cell void size feature shows that well-differentiated instances tend to have larger inter-cell void sizes. This observation can be explained by the scarcity of inter-cell voids in poorly-differentiated examples, and when they are present, they are usually smaller in size. It is to be noted that large inter-cell voids in the culture doesn't always mean better differentiation. For example, the presence of a single large inter-cell voids in the culture would signify poor differentiation. On the other hand, many evenly sized inter-cell voids throughout the culture signifies a standard differentiation.

Table 2 and Table 3 present the average values of performance metrics for images magnified 4 times (4X) and 10 times (10X) respectively. The performance metrics are for both unbalanced dataset as well as for dataset balanced by oversampling. For both unbalanced and balanced dataset, the model's performance is slightly better for 4X images compared to 10X images. Oversampling does not have a significance impact on the performance metrics for 4X and 10X image datasets.

Accuracy, which measures the proportion of correct predictions made by the model, shows that 10X magnified images have an average accuracy of 0.89, and 4X magnified images have an accuracy if 0.94 indicating that the model performs better for 4X images when it comes to accuracy. Recall, also known as sensitivity, measures the proportion of actual positives that are correctly identified. The average recall is higher for 4X images (0.82) compared to 10X images (0.87), suggesting that the model is better at identifying positive cases in 4X images. The metric precision measures the proportion of positive identifications that are actually correct. The average precision is higher for 4X images (0.97) than for 10X images (0.80), indicating that the model is more precise in its predictions for 4X images. The F1 score is a measure of a test's accuracy that considers both precision and recall. The average F1 score is higher for 4X images (0.91) compared to 10X images (0.80). This suggests that the model performs slightly better on 4X images when both precision and recall are considered.

The ROC-AUC score, which measures the area under the receiver operating characteristic (ROC) curve, is another important metric. The ROC curve is a plot that illustrates the diagnostic ability of a binary classifier system as its discrimination threshold is varied. The AUC (Area Under The Curve) represents the measure of separability, telling how much the model is capable of distinguishing between classes. The higher the AUC, the better the model is at predicting 0s as 0s and 1s as 1s. The average ROC-AUC score is higher for 4X images (0.97) than for 10X images (0.88), indicating that the model performs better on 4X images when distinguishing between the classes.

These performance metrics provide a comprehensive assessment of the model's performance on both 4X and 10X magnified images. The model's performance does not have a considerable difference between 10X and 4X magnified images. Best parameters estimated for 4X images were C=0.1, gamma = 1 and kernal as sigmoid. Best parameters estimated for 10X images was C=10, gamma =1 and kernal to be radial basis function. In SVM, the kernel transforms data into a higher dimension for complex decision boundaries, C establishes balance between low error on training data and decision function simplicity, and gamma influences the shape of the decision boundary. The difference in hyperparameters show that the model needs to be tuned for different magnifications.

For the 4X images, oversampling slightly improves the recall but reduces the accuracy and F1 score. For the 10X images, oversampling slightly improves the ROC-AUC and recall but reduces accuracy, F1 score and precision. These results suggest that oversampling may be slightly beneficial compared imbalanced dataset PCM images for some metcis but the difference in values are not very significant. Therefore, the performance of oversampling remains inconclusive and in the future this can be addressed by increasing the size of the dataset and balancing it which might help achieve higher accuracy.

5. CONCLUSION

In this paper, we present our preliminary findings of a non-invasive quality control method for bioreactors that uses PCM images for classification. Our model performs well on 4X and 10X validation sets, but we still have to establish

better correlation, and testing across different imaging systems is required to establish its robustness. The method promises to be more efficient and scalable compared to conventional lab methods and can be applicable in an online setting in bio-reactors for quality monitoring.

ACKNOWLEDGEMENTS

This research has been funded by the Médicament Québec. The research group acknowledged for the support. The authors would like to thank Josh Chang for his valuable comments and suggestions to improve the quality of the paper.

REFERENCES

Aigha, I.I. and Abdelalim, E.M. (2020). Nkx6. 1 transcription factor: a crucial regulator of pancreatic β cell development, identity, and proliferation. *Stem Cell Research & Therapy*, 11(1), 1–14.

Aigha, I.I., Memon, B., Elsayed, A.K., and Abdelalim, E.M. (2018). Differentiation of human pluripotent stem cells into two distinct nkx6. 1 populations of pancreatic progenitors. *Stem Cell Research & Therapy*, 9(1), 1–11.

Almezel, N.A. (2021). Stem cell production: Scale up, gmp production, bioreactor. *Advances in Application of Stem Cells: From Bench to Clinics*, 243–267.

Armi, L. and Fekri-Ershad, S. (2019). Texture image analysis and texture classification methods-a review. *arXiv preprint arXiv:1904.06554*.

Berrar, D. et al. (2019). Cross-validation.

Buades, A., Coll, B., and Morel, J.M. (2011). Non-local means denoising. *Image Processing On Line*, 1, 208–212.

Chan, T.H., Jia, K., Gao, S., Lu, J., Zeng, Z., and Ma, Y. (2015). Pcanet: A simple deep learning baseline for image classification? *IEEE transactions on image processing*, 24(12), 5017–5032.

Chauhan, V.K., Dahiya, K., and Sharma, A. (2019). Problem formulations and solvers in linear svm: a review. *Artificial Intelligence Review*, 52(2), 803–855.

Chawla, N.V., Bowyer, K.W., Hall, L.O., and Kegelmeyer, W.P. (2002). Smote: synthetic minority over-sampling technique. *Journal of artificial intelligence research*, 16, 321–357.

Docherty, F.M. and Sussel, L. (2021). Islet regeneration: endogenous and exogenous approaches. *International Journal of Molecular Sciences*, 22(7), 3306.

He, L., Ren, X., Gao, Q., Zhao, X., Yao, B., and Chao, Y. (2017). The connected-component labeling problem: A review of state-of-the-art algorithms. *Pattern Recognition*, 70, 25–43.

Kahan, B.W., Jacobson, L.M., Hullett, D.A., Ochoada, J.M., Oberley, T.D., Lang, K.M., and Odorico, J.S. (2003). Pancreatic precursors and differentiated islet cell types from murine embryonic stem cells: an in vitro model to study islet differentiation. *Diabetes*, 52(8), 2016–2024.

Kapoor, L. and Thakur, S. (2017). A survey on brain tumor detection using image processing techniques. In *2017 7th international conference on cloud computing, data science & engineering-confluence*, 582–585. IEEE.

Li, Q., Cai, W., Wang, X., Zhou, Y., Feng, D.D., and Chen, M. (2014). Medical image classification with convolutional neural network. In *2014 13th international conference on control automation robotics & vision (ICARCV)*, 844–848. IEEE.

Liu, D.Y., Gan, T., Rao, N.N., Xing, Y.W., Zheng, J., Li, S., Luo, C.S., Zhou, Z.J., and Wan, Y.L. (2016). Identification of lesion images from gastrointestinal endoscope based on feature extraction of combinational methods with and without learning process. *Medical image analysis*, 32, 281–294.

Maddalena, L. and Antonelli, L. (2024). Algorithms for biomedical image analysis and processing.

Maetschke, S., Tennakoon, R., Vecchiola, C., and Garnavi, R. (2017). Nuts-flow/ml: data pre-processing for deep learning. *arXiv preprint arXiv:1708.06046*.

Manohar, S., Shah, P., and Nair, A. (2021). Flow cytometry: principles, applications and recent advances. bioanalysis 13, 181–198.

Nicotra, T., Desnos, A., Halimi, J., Antonot, H., Reppel, L., Belmas, T., Freton, A., Stranieri, F., Mebarki, M., Larghero, J., et al. (2020). Mesenchymal stem/stromal cell quality control: validation of mixed lymphocyte reaction assay using flow cytometry according to ich q2 (r1). *Stem Cell Research & Therapy*, 11(1), 1–10.

Pagliuca, F.W., Millman, J.R., Gürtler, M., Segel, M., Van Dervort, A., Ryu, J.H., Peterson, Q.P., Greiner, D., and Melton, D.A. (2014). Generation of functional human pancreatic β cells in vitro. *Cell*, 159(2), 428–439.

Roy, P., Dutta, S., Dey, N., Dey, G., Chakraborty, S., and Ray, R. (2014). Adaptive thresholding: A comparative study. In *2014 International conference on control, Instrumentation, communication and Computational Technologies (ICCICCT)*, 1182–1186. IEEE.

Vaes, B., Craeye, D., and Pinxteren, J. (2012). Quality control during manufacture of a stem cell therapeutic. *BioProcess Int*, 10(S3), 50–55.

Van der Walt, S., Schönberger, J.L., Nunez-Iglesias, J., Boulogne, F., Warner, J.D., Yager, N., Gouillart, E., and Yu, T. (2014). scikit-image: image processing in python. *PeerJ*, 2, e453.

Vapnik, V. (1999). *The nature of statistical learning theory*. Springer science & business media.

Visschedijk, M., Hendriks, R., and Nuyts, K. (2005). How to set up and manage quality control and quality assurance. *The Quality Assurance Journal: The Quality Assurance Journal for Pharmaceutical, Health and Environmental Professionals*, 9(2), 95–107.

Wallner, K., Pedroza, R.G., Awotwe, I., Piret, J.M., Senior, P.A., Shapiro, A.J., and McCabe, C. (2018). Stem cells and beta cell replacement therapy: a prospective health technology assessment study. *BMC Endocrine Disorders*, 18, 1–12.

Wang, Q., Xie, J., Zuo, W., Zhang, L., and Li, P. (2020). Deep cnns meet global covariance pooling: Better representation and generalization. *IEEE transactions on pattern analysis and machine intelligence*, 43(8), 2582–2597.

Zhang, Y., Wang, X., Pong, M., Chen, L., and Ye, Z. (2017). Application of bioreactor in stem cell culture. *Journal of Biomedical Science and Engineering*, 10(11), 485–499.